

Mass Measurements of Focal Adhesions in Single Cells Using High Resolution Surface Plasmon Resonance Microscopy

Alexander W. Peterson*, Michael Halter, Alessandro Tona, Anne L. Plant, and John T. Elliott
Biosystems and Biomaterials Division, National Institute of Standards and Technology, 100 Bureau
Dr., Gaithersburg, MD 20899

ABSTRACT

Surface plasmon resonance microscopy (SPRM) is a powerful label-free imaging technique with spatial resolution approaching the optical diffraction limit. The high sensitivity of SPRM to small changes in index of refraction at an interface allows imaging of dynamic protein structures within a cell. Visualization of subcellular features, such as focal adhesions (FAs), can be performed on live cells using a high numerical aperture objective lens with a digital light projector to precisely position the incident angle of the excitation light. Within the cell-substrate region of the SPRM image, punctate regions of high contrast are putatively identified as the cellular FAs. Optical parameter analysis is achieved by application of the Fresnel model to the SPRM data and resulting refractive index measurements are used to calculate protein density and mass. FAs are known to be regions of high protein density that reside at the cell-substratum interface. Comparing SPRM with fluorescence images of antibody stained for vinculin, a component in FAs, reveals similar measurements of FA size. In addition, a positive correlation between FA size and protein density is revealed by SPRM. Comparing SPRM images for two cell types reveals a distinct difference in the protein density and mass of their respective FAs. Application of SPRM to quantify mass can greatly aid monitoring basic processes that control FA mass and growth and contribute to accurate models that describe cell-extracellular interactions.

Keywords: Surface plasmon, SPRM, focal adhesions, mass, density, cells, proteins

*alexander.peterson@nist.gov; phone 1 301 975-5665;

1. INTRODUCTION

Focal adhesions (FAs) are specialized multi-component protein complexes that permit communication between the interior of the cell and the extracellular matrix via integrin receptors and the actin cytoskeleton [1]. FAs contain many known proteins [2] and are involved in mechanical and chemical signaling. FA signaling is involved in a variety of cellular functions such as cell growth, morphogenesis, and cancer metastasis [3, 4]. Fluorescence microscopy is a primary tool used to quantitatively study FA morphology and dynamics [5]. This either requires immunofluorescent labelling of FAs or FAs with attached fluorescent labels. Therefore, only specifically labelled FA components can be visualized. Total internal reflection fluorescence microscopy (TIRFM) is one method used to create high resolution FA images [6]. The TIRFM evanescent wave is used to selectively probe fluorescence near the cell-substrate interface, allowing access to FA protein nanoarchitecture which resides well within 150 nm of the surface [7].

A technique such as surface plasmon resonance microscopy (SPRM) has the potential to be a useful orthogonal technique to that of fluorescence microscopy. It is a label-free surface sensitive imaging technique that uses conventional microscopy objectives to provide a mass and density measurement for FAs. This type of measurement fundamentally integrates all the protein assembly processes occurring in the FA growth process. Surface plasmon resonance (SPR) essentially measures the refractive index of a material at a thin metal surface [8]. The resonance minimum of SPR is sensitive to material near the surface and has the sensitivity to detect changes in surface protein binding [9]. SPR imaging is an approach to SPR that provides the ability to monitor spatial changes in reflectivity at an angle that is close to the resonance minimum [10]. These reflectivity values of the SPR image can be converted into index of refraction values by using the Fresnel model. SRPM is an extension of SPR imaging through a high numerical objective [11]. It provides the advantage of high magnification and compatibility with other microscopic imaging techniques. However, achieving the necessary spatial resolution needed to visualize subcellular features has been elusive until recently.

We have developed an SPRM system that is ideally suited to measuring subcellular components such as focal adhesions [12]. Essentially, an incident arc of light, shaped by a digital light projector, illuminates a gold coated coverslip through a high NA microscope objective at a selected excitation angle and captures the reflected image on a CCD camera. By limiting the angle of excitation light, the SPR signal to noise ratio is enhanced and this allows near-diffraction limited lateral resolution with 150 nm penetration depth above the substrate. This spatial resolution enables visualization of subcellular organelles, such as cellular focal adhesions. Obtaining SPRM images through a high NA objective requires us to correct for optical aberrations prior to using the Fresnel model which provides optical parameters such as index of refraction [13]. Here we interpret cellular focal adhesions as an optical layer and measure the index of refraction, which we convert into a protein density. The differences in focal adhesion properties between two different cell lines were examined with the SPRM system.

2. METHODOLOGY

Disclaimer: Certain commercial equipment, instruments, or materials are identified here in order to specify the experimental procedure adequately. Such identification is not intended to imply recommendation or endorsement by the National Institute of Standards and Technology, nor is it intended to imply that the materials or equipment identified are necessarily the best available for the purpose.

2.1 SPR Microscopy

The details of the apparatus are described previously [12, 13]. Briefly, we performed SPR on an inverted microscope (Olympus IX-70, Center Valley, PA) with a high numerical aperture objective lens (100 \times , 1.65 NA, Olympus) by launching an arc of 590 nm incident light using a digital light projector at the SPR imaging angle through the objective and collecting the reflected light image onto a CCD camera.

2.2 Substrate Preparation

The details of substrate preparation have been described previously [12]. Essentially, specialized coverslips (18 mm diameter, $n = 1.78$, Olympus) were coated with ≈ 1 nm chromium and ≈ 45 nm gold. The gold coated coverslip was immersed in a 0.5 mmol/L hexadecanethiol solution in ethanol for 12 h to generate a self-assembled monolayer. The coverslip was then inserted into a sterile solution of 25 $\mu\text{g}/\text{mL}$ bovine plasma fibronectin (Sigma, St. Louis, MO) in Ca^{2+} - and Mg^{2+} - free Dulbecco's phosphate buffered saline (DPBS; Invitrogen, Carlsbad, CA) for 1 h.

2.3 Cell Culture

The rat aortic vascular smooth muscle cell line, A10 (ATCC, Manassas, VA) was maintained in Dulbecco's Modified Eagles Medium with 25 mM HEPES (DMEM; Mediatech, Herndon, VA) supplemented with nonessential amino acids, glutamine, penicillin (100 units/mL), streptomycin (100 $\mu\text{g}/\text{mL}$), 10 % (v/v) fetal bovine serum (FBS) (Invitrogen); the human lung carcinoma cell line A549 (ATCC) was maintained in RPMI medium (Invitrogen) supplemented with glutamine, penicillin (100 units/mL), streptomycin (100 $\mu\text{g}/\text{mL}$), 10 % (v/v) FBS (Invitrogen); Both cell lines were maintained in a humidified 5 % (v/v) CO_2 balanced-air atmosphere at 37 $^\circ\text{C}$. Cells were harvested with 0.25 % (w/v) trypsin-EDTA (Invitrogen), and seeded in growth medium onto the fibronectin coated substrates at a density of 1000 cells/ cm^2 . After 72 h incubation, cells on the substrates were washed with warm Hanks Balanced Salt Solution (HBSS; ICN Biomedicals, Costa Mesa, CA), fixed in 1 % (w/v) paraformaldehyde (EMS, Hatfield, PA) in Dulbecco's phosphate buffered saline (DPBS; Invitrogen) for 30 min at room temperature, quenched in 0.25 % (w/v) NH_4Cl in DPBS (15 min) and rinsed with DPBS. The substrates were then overlaid with a fluidic chamber made out of polydimethylsiloxane (PDMS) and kept in DPBS during all microscopy measurements.

2.4 SPRM Image Collection and Processing

A SPRM image is created with a p- and s-polarized image taken by rotating the linear polarizer 90 $^\circ$ while using the arc-shaped incident illumination at an angle near the SPR minimum. The p-polarized image is divided by the s-polarized image to create a reflectivity image. The p/s intensities for each pixel are then divided by the apodization correction factor, which is a function of the calculated incident angle [13]. The result is an image with normalized and corrected reflectivity units. The images are further modified to convert the reflectivity units into Δ -reflectivity (ΔR) by using $\Delta R = R_1 - R_0$ where R_1 is the normalized reflectivity unit of the sample and R_0 is the average reflectivity of the SPR image

background in phosphate buffered saline (PBS) buffer. For subsequent analysis and comparison, the ΔR units are converted to index of refraction units according to the Fresnel model as described previously [13]. All image analysis was performed using ImageJ software with additional custom script programming. Angle-dependent SPR data were analyzed using stock and custom code written in MATLAB (Mathworks, Natick, MA).

2.5 Fluorescence Staining and Image Collection

After SPR imaging, the previously fixed substrates were permeabilized with 0.05 % (v/v) Triton X-100 (Sigma) in phosphate buffered saline (PBS) for 10 minutes at room temperature and blocked in 10 % (v/v) goat serum/1 % (w/v) bovine serum albumin in PBS (blocking solution) for 30 minutes at room temperature. The samples were then stained with monoclonal anti-vinculin antibody (Sigma) diluted 1:200 in blocking solution for 1 hour at room temperature. After rinsing 3 \times with PBS and blocking again with blocking solution for 30 minutes at room temperature, the samples were stained with Alexa-488 goat anti-mouse secondary antibody (Invitrogen) diluted 1:100 in blocking solution for 45 minutes at room temperature. Finally, the samples were rinsed 3 \times in PBS and stored in PBS for imaging. Fluorescence images were acquired with a 1.3 NA, 63 \times objective on an upright Zeiss microscope (Zeiss, Jena, Germany) using a standard FITC filter cube set. Each fluorescence image was registered to the corresponding SPR image using 2 fiduciary marks according to the TurboReg plugin in the ImageJ software.

2.6 Focal Adhesion Image Analysis

Fluorescently stained α -vinculin images were processed and analyzed for FA area measurements using ImageJ software according to a published method [14]. The overlays generated by the α -vinculin FA analysis were used to guide the manual threshold selection for the corresponding SPRM image. The average change in reflectivity for each FA area in a SPRM image is converted into a change in refractive index as previously described [13] and then converted into mass density according to the specific refractive index increment (0.18 mL/g) for biomolecules widely used in optical live-cell mass profiling techniques [15]. The terminology typically used for optical mass measurements refers to 'dry mass' as the mass of all biomolecular components other than water. Here, our interpretation is analogous as we measure refractive index shifts compared to buffered media, however, we have adopted the nomenclature 'protein mass' and 'protein density' to describe the multi-protein component structures of FAs. The protein density value for each FA (in units of fg/ μm^3) is then converted into protein mass by multiplying the measured lateral FA area (μm^2) and the measured axial penetration depth of the surface plasmon (0.15 μm) [12]. ≈ 450 FAs were measured for A549 cells, and ≈ 600 FAs were measured for A10 cells. The basal cell mass density is calculated by averaging the SPRM contrast attributed to the footprint of the cell minus the area of regions attributed to FAs. This is done as a per cell measurement with 9 cells each.

3. RESULTS AND DISCUSSION

3.1 SPRM Technique and Focal Adhesion Size

The details of our surface plasmon resonance microscopy (SPRM) apparatus has been described previously [12, 13]. Briefly, an incident arc of light at 590 nm is shaped by a digital light projector to illuminate the SPR imaging angle through a microscope objective off a gold coated coverslip and capture the reflected image onto a CCD camera (Figure 1A). This provides diffraction-limited spatial resolution for SPR imaging of cellular samples. The image contrast in reflectivity units can be converted into index of refraction units using the Fresnel model [13]. Here, we apply SPRM to quantitatively analyze cellular focal adhesions (FA) by converting index of refraction units into protein density by using the refractive index increment used for biomolecular components [15]. Subsequently, we can measure the protein mass of FAs by multiplying the measured protein density value by the measured lateral area of the FA and the previously measured axial distance of the SPR penetration depth.

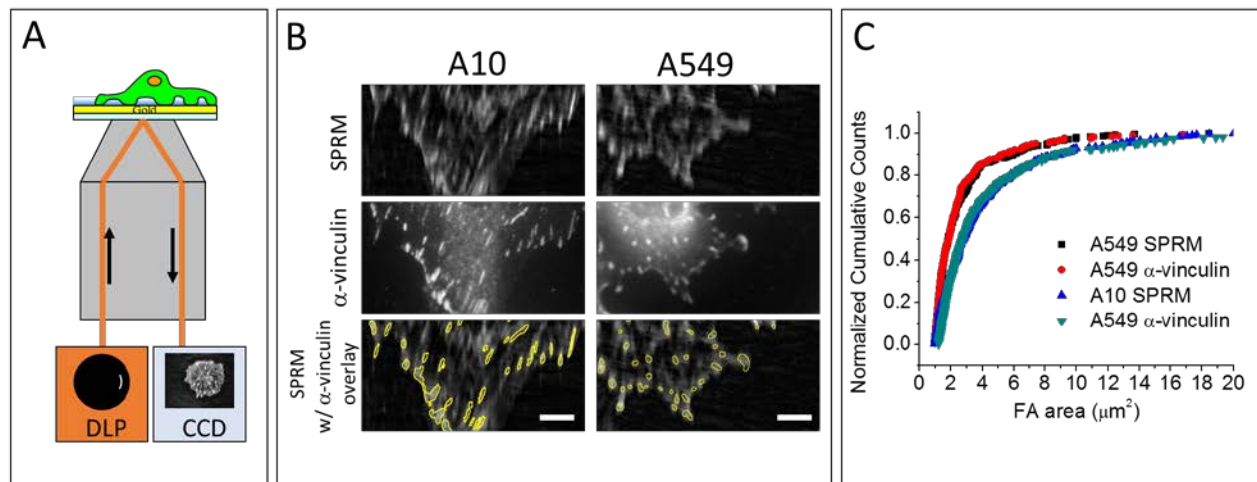


Figure 1: Surface plasmon resonance microscopy (SPRM) of A10 and A549 cellular focal adhesions (FA) show similar area measurements as that for fluorescently stained α -vinculin. A) Simplified SPRM schematic depicting an incident arc of light at the SPRM imaging angle through a microscope objective and resulting SPRM image captured on a CCD camera. B) SPRM images of an A10 and A549 cell, same cells subsequently labelled with α -vinculin and fluorescently imaged, intensity threshold of α -vinculin overlaid onto corresponding SPRM image for comparison. Scale bar = 10 μm . C) Normalized cumulative counts plots for FA area showing similar distributions for SPRM and fluorescently stained α -vinculin for each cell type, with distinct median values of 2.7 μm^2 for A10 and 1.8 μm^2 for A549 cells.

Two cell types, vascular smooth muscle cells (A10) and adenocarcinomic alveolar basal epithelial cells (A549) were seeded and fixed after 72 h on a fibronectin coated substrate as described in Methodology 2.3. The SPRM images of representative A10 and A549 cells show regions of high optical contrast that are directly related to the mass density of the cellular components within the evanescent wave (Figure 1B). For comparison, immunofluorescently labeled α -vinculin, a known focal adhesion associated protein, is displayed next to the SPRM image to visualize the cellular FAs. The bottom combination images depict the outline of a threshold performed on the fluorescence images of α -vinculin overlaid on the SPRM images. From these images, we can observe that the bright punctate regions in the SPR image match well with the α -vinculin stained regions and therefore SPRM is likely detecting FAs as regions of higher protein density. Image analysis was used to measure FA area for α -vinculin fluorescent images of A10 and A549 cells to help guide the manual thresholding of the FAs in the SPRM images. Comparing the cumulative counts of FA areas between SPRM and α -vinculin images and between A10 and A549 cells, it is revealed that SPRM can closely match the FA area distribution profile for α -vinculin, and that there is an observable difference in FA area between A10 and A549 cells. The median FA area for A10 cells is 2.7 μm^2 and 1.8 μm^2 for A549 cells. A10 cells are known to have large FAs on stiff substrates [16] and A549 cells are described as having substantially smaller FAs than normal cells [17].

3.2 Focal Adhesion Protein Density

Using the outlined FA areas for A10 and A549 cells with SPRM, the protein density for each FA is calculated as described above. In addition, the basal cell surface, the area of SPRM cellular contrast that corresponds to cellular area, minus the areas attributed to FA area, is averaged to calculate a basal cell mass density. Consequently, the average protein densities and standard deviations for the A10 and A549 FAs, and basal cell areas are compared (Fig. 2A) revealing that FAs in A10 cells have nearly twice the protein density as FAs in A549 cells. In addition, the protein densities of FAs in both cell types are significantly larger than the basal cell background densities which represents the mass density of the general cytoplasm ($p < 0.0001$).

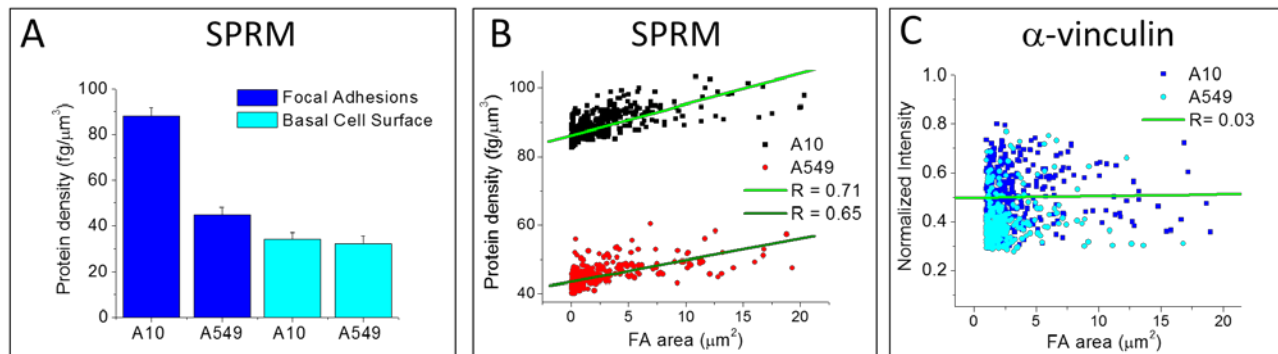


Figure 2: SPRM measured protein densities for focal adhesions of A10 and A549 cells show an increase in protein density with an increase in FA area. A) FA protein density values reported show A10 FAs are significantly denser than A549 FAs. Both cell type FAs have larger densities than that of the basal cells surfaces which have similar lower densities. B) FA protein density for A10 and A549 cells show a strong correlation with FA area ($R=0.71$ for A10, $R=0.65$ for A549). C) Normalized fluorescence intensity for α -vinculin shows no observable correlation with FA area ($R=0.03$ for A10, $R=0.10$ for A549 (fit not shown)).

In contrast, basal cell mass densities of A10 and A549 cells are statistically similar ($p > 0.65$). Protein densities of FAs for both A10 and A549 cells show a strong correlation ($R=0.71$ for A10, $R=0.65$ for A549) when plotted versus FA area, Figure 2B. This correspond to $\approx 1 \text{ fg}/\mu\text{m}^2$ gain in protein density per $1 \mu\text{m}^2$ of FA area for A10 cells while half of that value for A549 cells. In contrast, fluorescence intensity of α -vinculin FAs plotted versus FA area reveals no correlation ($R=0.03$ for A10, $R=0.10$ for A549), Figure 2C. A possible explanation is that, in the case for α -vinculin, it is a FA associated protein that has been measured to reside in a specific plane of the FA [7], therefore it would not be predicted to change in density along with FA size, rather it will remain at constant density. However, other FA associated proteins, such as actin stress fibers, may occupy more volume in the FA [7] and may be more dynamic in abundance and density in the FA. Actin fibers in A10 cells are described as expanding when cells are on stiff substrates [16] and actin fibers are described as diminished in A549 cells compared to normal cells [17]. Regardless, SPRM measures the integrated overall protein density and large differences are observed in protein density between FAs of different cells types as well as smaller differences in FA protein density as a function of FA area.

3.3 Focal Adhesion Protein Mass

Protein mass measurements of FAs are measured by multiplying the average protein density of the FA by the volume of the FA. In our case, the volume of FA is the measured FA area multiplied by the length of the SPR penetration depth into the cell. Observing the cumulative counts of FA mass for A10 and A549 cells reveals a distinct distribution for each cell type, where the median mass for A10 FAs is 46 fg while the median mass for A549 FAs is 19 fg, Figure 3A.

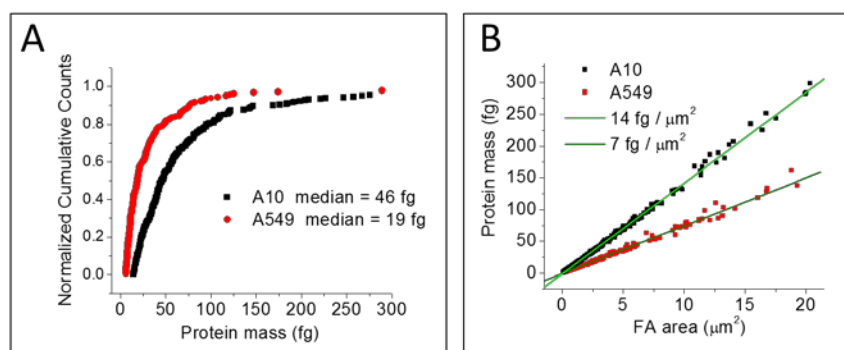


Figure 3: Focal adhesion protein mass measurements show that A10 FAs have significantly more mass than FAs for A549 cells. A) Normalized cumulative distribution plot for FA protein mass shows a median value of 46 fg for A10 cells and 19 fg for A549 cells. B) FA protein mass plotted versus FA area shows a strong positive correlation ($R=0.99$) for A10 and A549 cells. The slope of a linear fit reports a larger mass gain of $14 \text{ fg}/\mu\text{m}^2$ of FA area for A10 cells compared to $7 \text{ fg}/\mu\text{m}^2$ of FA area for A549 cells.

The separation in these mass distributions appears to be more distinct than that of FA area alone, Figure 1C. Evaluating FA protein mass versus FA area shows a strong correlation between FA protein mass and FA size for both A10 and A549 cells, Figure 3B. However, the measured slopes of protein mass versus FA area show distinct values of $14 \text{ fg}/\mu\text{m}^2$ for A10 FAs and $7 \text{ fg}/\mu\text{m}^2$ for A549 cells. The large differences in FA protein mass between these cell types may be due to the presence or absence of certain FA components, such as actin stress fiber attachments. The strong linear correlation of FA protein mass with FA area may indicate a level of homogeneity in FA growth response. Additionally, both A10 and A549 cells grown on flat, stiff, fibronectin coated surfaces were non-motile cells which may contribute to more homogenous FA area and mass response.

4. CONCLUSION

We have created a SPRM system that can obtain near-diffraction lateral resolution and has an evanescent wavelength of 150 nm that is able to visualize, label-free, subcellular components, such as FAs, and is ideally suited to make quantitative measurements of FA protein density and mass. The protein density and mass measurements on FAs show distinct differences between FAs for two different cells types. These protein mass measurements are tied to biophysical processes that have significant meaning for understanding of FA formation and development. The results here are very promising and continued work will be on evaluating FA dynamics in live-cells.

REFERENCES

- [1] S. K. Sastry, and K. Burridge, "Focal adhesions: A nexus for intracellular signaling and cytoskeletal dynamics," *Experimental Cell Research*, 261(1), 25-36 (2000).
- [2] K. Burridge, and M. Chrzanowska-Wodnicka, "Focal adhesions, contractility, and signaling," *Annual Review of Cell and Developmental Biology*, 12, 463-518 (1996).
- [3] B. Geiger, J. P. Spatz, and A. D. Bershadsky, "Environmental sensing through focal adhesions," *Nature Reviews Molecular Cell Biology*, 10(1), 21-33 (2009).
- [4] M. A. Schwartz, M. D. Schaller, and M. H. Ginsberg, "Integrins: Emerging paradigms of signal transduction," *Annual Review of Cell and Developmental Biology*, 11, 549-599 (1995).
- [5] M. E. Berginski, E. A. Vitriol, K. M. Hahn *et al.*, "High-Resolution Quantification of Focal Adhesion Spatiotemporal Dynamics in Living Cells," *Plos One*, 6(7), (2011).
- [6] A. L. Mattheyses, S. M. Simon, and J. Z. Rappoport, "Imaging with total internal reflection fluorescence microscopy for the cell biologist," *Journal of Cell Science*, 123(21), 3621-3628 (2010).
- [7] P. Kanchanawong, G. Shtengel, A. M. Pasapera *et al.*, "Nanoscale architecture of integrin-based cell adhesions," *Nature*, 468(7323), 580-U262 (2010).
- [8] J. Homola, [Surface Plasmon Resonance Based Sensors] Springer, Berlin(2006).
- [9] D. Altschuh, M. C. Dubs, E. Weiss *et al.*, "Determination of Kinetic Constants for the Interaction between a Monoclonal-Antibody and Peptides Using Surface-Plasmon Resonance," *Biochemistry*, 31(27), 6298-6304 (1992).
- [10] L. K. Wolf, D. E. Fullenkamp, and R. M. Georgiadis, "Quantitative angle-resolved SPR imaging of DNA-DNA and DNA-drug kinetics," *J Am Chem Soc*, 127(49), 17453-17459 (2005).
- [11] B. Huang, F. Yu, and R. N. Zare, "Surface plasmon resonance imaging using a high numerical aperture microscope objective," *Analytical chemistry*, 79(7), 2979-2983 (2007).
- [12] A. W. Peterson, M. Halter, A. Tona *et al.*, "High resolution surface plasmon resonance imaging for single cells," *BMC Cell Biol*, 15, 35 (2014).
- [13] A. W. Peterson, M. Halter, A. L. Plant *et al.*, "Surface plasmon resonance microscopy: Achieving a quantitative optical response," *Review of Scientific Instruments*, 87(9), (2016).

- [14] U. Horzum, B. Ozdil, and D. Pesen-Okvur, "Step-by-step quantitative analysis of focal adhesions," *MethodsX*, 1, 56-9 (2014).
- [15] T. A. Zangle, and M. A. Teitell, "Live-cell mass profiling: an emerging approach in quantitative biophysics," *Nature Methods*, 11(12), 1221-1228 (2014).
- [16] A. L. Plant, K. Bhadriraju, T. A. Spurlin *et al.*, "Cell response to matrix mechanics: Focus on collagen," *Biochimica Et Biophysica Acta-Molecular Cell Research*, 1793(5), 893-902 (2009).
- [17] M. M. Alam, J. Hooda, D. Cadinu *et al.*, "Comparative proteomic analysis of an isogenic pair of lung normal and lung cancer cell line," *Faseb Journal*, 27, (2013).